

THE INITIAL TRANSIENT BEHAVIOR OF A THERMOELECTRIC GENERATOR

by

FERREL GERBEN STREMLER

A.B., Calvin College
(1957)

B.S., Illinois Institute of Technology
(1959)

SUBMITTED IN PARTIAL FULFILLMENT OF THE
REQUIREMENTS FOR THE DEGREE OF
MASTER OF SCIENCE

at the

MASSACHUSETTS INSTITUTE OF TECHNOLOGY
September, 1960

Signature of Author
Department of Electrical Engineering, August 22, 1960

Certified by _____ Thesis Supervisor

Accepted by _____
Chairman, Departmental Committee on Graduate Students

THE INITIAL TRANSIENT BEHAVIOR OF A THERMOELECTRIC GENERATOR

by

Ferrel Gerben Stremier

Submitted to the Department of Electrical Engineering on August 22, 1960, in partial fulfillment of the requirements for the degree of Master of Science.

ABSTRACT

The basic mathematical relations in the thermoelectric generator are described for the assumptions that the flow of heat is essentially one-dimensional, the elements of the device are homogeneous, and the parameters of the system are independent of the temperature. On the basis of these equations and an energy balance for the system, a relation between the junction temperatures and the current output of the device is derived. This latter result reduces the problem of computing the initial current transient to that of finding a solution for the temperature of the junctions as a function of time. The specific case considered corresponds to applying a step of heat to the hot junction of the device which is in thermal equilibrium with its surroundings and finding the output current as a function of time for a constant cold junction temperature.

The equations considered are non-linear in terms of the current and the current-temperature product. This makes it necessary to appeal to a perturbative-type solution where the initial or unperturbed solution is simply the solution for zero current. This method takes advantage of the fact that the efficiency of such a device is quite low so that any perturbations to a general solution will converge rapidly. The solutions for zero current and for the first perturbation are derived on the assumption that the Thomson heat term is negligible and a test for the convergence of the perturbation is given. The results of the theory are compared with a practical model of the generator and are found to be in good overall agreement with the theory within the limits of the assumptions which were made. The constant parameter assumption introduces some error for the practical case and this is pointed out.

The results of this theory are simplified from practical considerations and these simplified results are applied to the problem of predicting the settling of the

system under the conditions previously mentioned. The results are compared with experimental values and are found to be in excellent agreement. This close agreement is attributed to the fact that the constant-parameter assumption holds very closely for this special case. Additional information concerning the experiment is included in the appendices.

Thesis Supervisor:

Dr. Paul E. Gray

Title:

Assistant Professor of Electrical Engineering

ACKNOWLEDGEMENT

The author wishes to thank Dr. P. E. Gray of the Department of Electrical Engineering for his suggestions, interest, and helpful advice in this work, both theoretical and in the laboratory. At times, when the problems seemed insurmountable, it was his advice and encouragement that furnished new insight.

Sincere appreciation is also expressed to the members and assistants of the Energy Conversion Laboratory who gave helpful advice and assistance in the experimental work and to my wife, Ruth, for the typing of the thesis.

TABLE OF CONTENTS

List of Figures and Tables	6
Introduction	7
I. Statement of the Problem	9
II. Transients in the Unloaded Generator	15
III. The Effect of a Load on the Transient Behavior	28
IV. The Settling Time of the System	41
Remarks	46
Appendix A: Details of the Experimental Model	49
Appendix B: Determination of the Average Parameters	53
Appendix C: A Partial List of Residues for the Complete Solution	58
References	60

LIST OF FIGURES AND TABLES

1-1	The Thermoelectric Generator	11
2-1	A Graphical Solution of the Transcendental Equation: $\text{Tangent } \alpha = \frac{1}{2x}$	23
2-2	The Residues for the Unperturbed Solution	24
2-3	Unperturbed Results for the Hot Junction Temperature	27
3-1	The Perturbations of the Junction Current	38
3-2	A Comparison of the Results with the Experiment	38
4-1	Device Settling Times for Constant Power Input	43
A-1	A Block Diagram of the Experiment	50
A-2	The Experimental Generator	50
A-3	Details of the Heater	51
B-1	The Effective α and κ of the Generator Arms	55
B-2	The Resistivity of the Bismuth Telluride Used	55
B-3	The Volt-Ampere Characteristic for a Constant Power Input	56
B-4	The Effective z of the Generator	56
C-1	The Numerical Results for the Residues of Eq. C-1	59

INTRODUCTION

The efficiency and the steady state behavior of the thermoelectric device have been treated in the literature.¹⁻³ More recently, considerable work has been done treating the transient behavior for incremental variations about a quiescent operating point.⁴ This procedure avoided the inherent nonlinearities of the problem by creating a linearized mathematical model, and the method can be extended to many problems for the small signal case. However, there are certain problems which this method will not handle, the main one of which is concerned with the large-signal dynamic behavior. A particularly important example is the problem of the start-up transient of a thermoelectric device under load. It is this problem to which this work is directed.

Until recent developments, the efficiency of the thermoelectric generator has been low and the questions of transient behavior have been secondary. As the efficiency continues to be improved, however, these problems become quite pertinent and important.

The problem of predicting the exact variation of the output current is treated first and then the important problem of device settling time is considered. Since the system is non-linear in terms of current, an iterative process is necessary for a solution. To employ such a process, we make use of the fact that the efficiency of

the device is low. This may seem to be paradoxical at first glance; however, the efficiency of present day devices has room for improvement before the method to be used will not converge.

I. STATEMENT OF THE PROBLEM

In 1822, Seebeck discovered the effect (which bears his name) that relates the open circuit voltage developed across a junction of two dissimilar materials to the temperature differential between the two materials. This Seebeck coefficient, α , can be defined in terms of the temperature and the open circuit terminal voltage:

$$\alpha = - \frac{dV}{dT} \quad (1.1)$$

If a current is passed through this junction, heat is generated or absorbed at the junction, depending upon the direction of the current flow. This effect was first observed by Peltier in 1834 and is expressed as:

$$Q_p = \pi I \quad (1.2)$$

where π is the Peltier coefficient. Later Thomson showed, by a thermodynamic analysis, the relationship between the Peltier and the Seebeck effects:*

$$\pi = \alpha T \quad (1.3)$$

T is the absolute temperature of the junction itself. (The Peltier effect is a phenomenon which takes place only at the junction between the two dissimilar materials.)

In addition to providing a tie between these two effects, Thomson predicted a third phenomenon which bears

* See, for instance, Ref. 1, p. 8 ff., or Ref. 2, pp. 4-6.

his name. This effect is defined as the generation or absorption of heat in the presence of an electric current and a temperature gradient:

$$Q_t = \tau I \frac{dT}{dx} \quad (1.4)$$

where τ is the Thomson coefficient and is related to the Seebeck and Peltier coefficients.* It is assumed that the conductor is homogeneous and that both the temperature gradient and the current flow are in the x direction only. For both the Peltier and the Thomson effects, the energy exchange between the system and the surroundings is reversed with a reversal of the direction of electric current flow. In contrast, the Joule heat is simply an energy dissipation.

The effects described above provide the basis for the development of the thermoelectric device. The Peltier effect is used to advantage for the thermoelectric cooler, whereas the thermoelectric generator makes use of the Seebeck effect. In this paper, we shall be concerned with the latter. For devices using good present-day materials, the Thompson effect and the Joule heat are of second order for the generator.

A basic device for the thermoelectric generation of power is shown in Figure 1-1. The device consists of one

* See Ref. 2, pp. 6-11. (This reference also gives a brief microscopic interpretation of these thermodynamic relations.)

p-type and one n-type semiconductor* to which the electrical and thermal connections are made by metallic contacts. These contacts are assumed, as a first approximation, to furnish ideal conductors to the "sinks".

In other words, they are assumed to have negligible specific heat and zero thermal and electrical resistivity. For the practical case, these assumptions can be made quite valid for steady state operation; however, the first assumption cannot be made for the transient case since the thermal mass of the connecting strap is non-zero and introduces

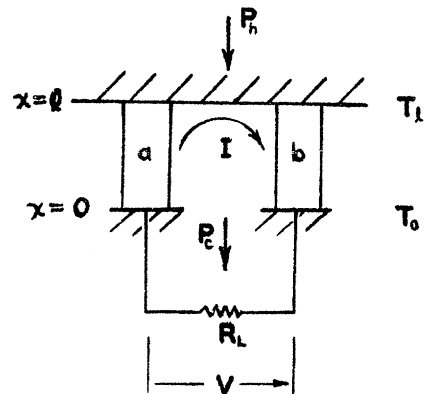


FIGURE I-1
THE THERMOELECTRIC
GENERATOR

an effect on the transient behavior of the system. We shall retain the latter two assumptions, namely, that the thermal and electrical resistivities are negligible.

Considerable work can be avoided by choosing convenient notation and normalizing factors at the outset. Much of the notation and the grouping of appropriate normalizing factors is due to the work of P. E. Gray to whom the author is indebted for his help. For further information on the notation used, the reader is referred to his work.⁴

* (labelled as elements a and b for simplicity of notation)

We shall define the parameters of the system as:

- ρ_a, ρ_b electrical resistivity of the elements
- κ_a, κ_b thermal conductivity of the elements
- c_a, c_b specific heat of the elements
- A_a, A_b element cross-sectional areas
- τ_a, τ_b Thompson coefficients of the elements
- α the equivalent differential thermoelectric coefficient
- c_o specific heat of the hot junction connecting strap
- A_o cross-sectional area of the hot junction connecting strap
- l_o axial length of the connecting strap

In this analysis, we shall assume that the flow of heat is essentially one-dimensional, the elements are assumed to be homogeneous, and the above parameters are assumed to be independent of the temperature. This last restriction is the most severe and, as we shall see later, introduces errors into the work. However, as is often the case, we are forced to make the assumptions to keep the problem simple enough to find a solution.

Referring to Figure 1-1, we can now make use of the parameters defined above to set up an energy balance for the system. The equations are the conventional ones and need no further comment. For the two arms, an incremental balance of heat flow and stored energy

yields:

$$\kappa_a A_a \frac{\partial^2 T_a}{\partial x^2} - r_a I \frac{\partial T_a}{\partial x} + \frac{\rho_a}{A_a} I^2 = c_a A_a \frac{\partial T_a}{\partial t} \quad (1.5)$$

$$\kappa_b A_b \frac{\partial^2 T_b}{\partial x^2} + r_b I \frac{\partial T_b}{\partial x} + \frac{\rho_b}{A_b} I^2 = c_b A_b \frac{\partial T_b}{\partial t} \quad (1.6)$$

For the entire system, we have the following energy balance:

$$P_h - P_c = I^2 R_L + \frac{\partial W}{\partial t} \quad (1.7)$$

where:

$$W = A_a \int_0^l c_a T_a dx + A_b \int_0^l c_b T_b dx \quad (1.8)$$

$$P_c = \alpha_o T_o I_o + \kappa_a A_a \left. \frac{\partial T_a}{\partial x} \right|_{x=0} + \kappa_b A_b \left. \frac{\partial T_b}{\partial x} \right|_{x=0} \quad (1.9)$$

$$P_h = \alpha_l T_l I + \kappa_a A_a \left. \frac{\partial T_a}{\partial x} \right|_{x=l} + \kappa_b A_b \left. \frac{\partial T_b}{\partial x} \right|_{x=l} + c_o A_o l_o \left. \frac{\partial T}{\partial t} \right|_{x=l} \quad (1.10)$$

This completes the description of the system excluding the external constraints. The constraints in which we are interested correspond to a device at equilibrium with the surroundings at $t=0^-$. At a given instant of time ($t=0$ for convenience) a step input of heat is applied to the hot junction ($x=l$) and the cold junction ($x=0$) is kept at the initial equilibrium temperature, T_o . Under these conditions it is desired to formulate the current output as a function of time under various load conditions. These conditions can therefore be summarized in the following manner:

$$T_1(0,t) = T_2(0,t) = T_o \quad (1.11)$$

$$T_1(l,t) = T_2(l,t) = T_l(t) \quad (1.12)$$

$$T_1(x, 0) = T_2(x, 0) = T_0 \quad (1.13)$$

$$P_h(t) = 1(t) W \quad (1.14)$$

where the notation $1(t)W$ is used to indicate a step of magnitude W watts and occurring at the instant $t=0$.

These equations form the mathematical description of the thermoelectric generator and hold for any constant parameter system where the system is homogeneous and one-dimensional. In the next chapter we shall further restrict the system before attempting to find a solution.

we have:

$$\kappa_a A_a \left. \frac{\partial T_a}{\partial x} \right|_{x=l} - \kappa_a A_a \left. \frac{\partial T_a}{\partial x} \right|_{x=0} - c_a A_a \int_0^l \frac{\partial T_a}{\partial t} dx + \frac{\rho_a}{A_a} I^2 l = 0 \quad (2.1)$$

$$\kappa_b A_b \left. \frac{\partial T_b}{\partial x} \right|_{x=l} - \kappa_b A_b \left. \frac{\partial T_b}{\partial x} \right|_{x=0} - c_b A_b \int_0^l \frac{\partial T_b}{\partial t} dx + \frac{\rho_b}{A_b} I^2 l = 0 \quad (2.2)$$

Differentiating Eq. 1.8 with respect to t gives:

$$\frac{\partial W}{\partial t} = c_a A_a \int_0^l \frac{\partial T_a}{\partial t} dx + c_b A_b \int_0^l \frac{\partial T_b}{\partial t} dx \quad (2.3)$$

Substituting the above relations and Eqs. 1.9 and 1.10 into Eq. 1.7 yields:

$$\alpha_1 T_1 I - \frac{\rho_a}{A_a} I^2 l - \frac{\rho_b}{A_b} I^2 l - \alpha_0 T_0 I = I^2 R_L \quad (2.4)$$

This is an important relation for the thermoelectric generator and holds for any constant parameter, homogeneous system where the heat flow is assumed to be one-dimensional and the Thomson heat is neglected. Making use of the definition:

$$R_{eq} \triangleq \left(\frac{\rho_a}{A_a} + \frac{\rho_b}{A_b} \right) l \quad (2.5)$$

where R_{eq} is the effective internal resistance of the device and also making the assumption that the connecting straps for the hot and cold junctions are constructed from the same material so that:

$$\alpha = \alpha_0 = \alpha_1 \quad (2.6)$$

Eq. 2.6 can be simplified to:

$$I = \frac{\alpha (T_1 - T_0)}{R_L + R_{eq}} \quad (2.7)$$

It will prove to be convenient to normalize the loading of the generator to the internal resistance by a dimen-

II. TRANSIENTS IN THE UNLOADED GENERATOR

The basic equations which describe the behavior of the device have been set up in Chapter I. Since the equations are non-linear in the current and the current-temperature products, the thought occurs to us to set the current equal to zero and solve for the temperature distribution under these conditions. If the efficiency of the system is low, the interaction could then be treated as a perturbation to the initial solution and, by such a perturbative procedure, the final value for current could be obtained. This method looks promising but first of all a relation between the current and the temperature across the device is found.

Before proceeding, however, we shall consider any simplifications to the equations of Chapter I. The simplification which we would like to make in Eqs. 1.5 and 1.6 is that the terms involving the first derivative of the temperature with respect to the space coordinate vanish. This simplifies the differential equations tremendously and, as mentioned in Chapter I, this corresponds closely to the practical case of the thermoelectric generator for many materials. Explicitly, then, we shall assume that the Thomson heat terms are negligible and therefore $\tau_s = \tau_c = 0$ is implied in all subsequent work.

By integrating Eqs. 1.5 and 1.6 with respect to x ,

sionless parameter such that:

$$m \triangleq \frac{R_L}{R_{eq}} \quad (2.8)$$

Then Eq. 2.7 becomes:

$$I = \frac{\alpha [T_L(t) - T_o]}{R_{eq} (m+1)} \quad (2.9)$$

This is the desired result that relates the output current of the device to the temperature difference across the arms. Eq. 2.9 has been derived making use of several assumptions; however, they are not unduly restrictive.

An examination of the boundary conditions listed in Chapter I and Eq. 2.9 reveals that it will be more convenient to refer all temperatures to the base temperature, T_o , so that

$$\bar{T} \triangleq T - T_o \quad (2.10)$$

Since the differential equations are all linear in terms of temperature, this change of variable does not affect the equations previously set forth* and the boundary conditions, Eqs. 1.11, 12, 13 now become:

$$\bar{T}_a(0, t) = \bar{T}_b(0, t) = 0 \quad (2.11)$$

$$\bar{T}_a(l, t) = \bar{T}_b(l, t) = \bar{T}_L(t) \quad (2.12)$$

$$\bar{T}_a(x, 0) = \bar{T}_b(x, 0) = 0 \quad (2.13)$$

and Eq. 2.9 simplifies to:

$$I = \frac{\alpha \bar{T}_L(t)}{R_{eq} (m+1)} \quad (2.14)$$

* In general, it might add a constant. It does not in this case, however, because the temperature enters the equations only as a derivative.

At this point we shall try to simplify the work by assuming that the parameters of the two arms are very similar so that they can be averaged. In particular, the parameters which we wish to average are the Seebeck coefficient, α , the electrical resistivity, ρ , and the thermal conductivity, κ . Although there are other ways in which these parameters can be averaged, we choose to average them by taking one half of the sum (the arithmetic mean) of each parameter value. In the case of α , the absolute values are used. For specific examples, the reader is referred to Appendix B. This approximation holds quite well for the case where the two arms are constructed of the same material but with different dopings (for example, p- and n-type bismuth telluride). This simplifies the analysis tremendously since now Eqs. 1.5 and 1.6 become identical and only one solution need be obtained. The solution for the case of two dissimilar arms does not require any new theory but the work is much more lengthy. As will be seen, the work for the case which we are considering becomes lengthy enough!

We can now proceed with the plan of attack mentioned at the beginning of this chapter. Since the equations considered are non-linear in terms of the current, a perturbative-type of solution is chosen. This method takes advantage of the fact that the efficiency of such a device is rather low so that any perturbations to a

general solution will converge rapidly. As a first approximation, then, we can solve for the temperature distribution for the case of $I=0$ and, from Eq. 2.14, find the current (fictitious) which would result from this temperature distribution if there were no other effects. By using this value for the current, and keeping it fixed at this value, a perturbed temperature distribution can be obtained to correct for the initial assumption.

To simplify the work as much as possible, we shall employ the conventional methods of the Laplace transformation to handle the time dependence and the conventional methods of differential equations to handle the space dependence. A working knowledge of both is assumed and many of the steps which involve these conventional techniques will be omitted in the interest of clarity and brevity.

By setting the current equal to zero, the equation for the temperature distribution becomes:

$$\kappa \frac{\partial^2 \bar{T}}{\partial x^2} = c \frac{\partial \bar{T}}{\partial t} \quad (2.15)$$

which results in a solution in the s domain of the form:

$$\bar{T}(x, s) = A e^{\delta x} + B e^{-\delta x} \quad (2.16)$$

where

$$\delta = \left[\frac{c}{\kappa} s \right]^{1/2} . \quad (2.17)$$

The boundary conditions for this system are given by Eqs. 1.10 and 1.14 which, for arms with average param-

eters and $I = 0$, becomes:

$$P_h = 1(t)W = 2\kappa A \left. \frac{\partial \bar{T}}{\partial x} \right|_{x=l} + c_o A_o l_o \left. \frac{\partial \bar{T}}{\partial t} \right|_{x=l} \quad (2.18)$$

where W is the magnitude of the heat input to the system in watts. If the connecting strap is constructed of copper or some other metal with high thermal conductivity, we can assume that the temperature gradient across the strap is negligible compared to that across the arms so that, transforming to the s domain:

$$2\kappa A \left. \frac{\partial \bar{T}}{\partial x} \right|_{x=l} = \frac{W}{s} - c_o A_o l_o s \bar{T}_l \quad (2.19)$$

where we have used the initial condition:

$$\bar{T}(x, 0) = 0 \quad (2.13)$$

or

$$\left. \frac{\partial \bar{T}}{\partial x} \right|_{x=l} = \frac{W}{2\kappa A s} - \frac{c_o A_o l_o}{2\kappa A} s \bar{T}_l \quad (2.20)$$

$$\left. \frac{\partial \bar{T}}{\partial x} \right|_{x=l} = \frac{W}{2\kappa A s} - \frac{t_c \bar{c}}{l} s \bar{T}_l \quad (2.21)$$

$$\text{where: } \bar{c} \triangleq \frac{c_o A_o l_o}{2\kappa A l} \quad (2.22)$$

$$t_c \triangleq \frac{\bar{c}}{\kappa} l^2 \quad (2.23)$$

The normalized parameter, \bar{c} , is the total specific heat of the hot junction connecting strap normalized to the total specific heat of the elements and t_c (the "characteristic time") is introduced here since it will be apparent later that the time response of the entire system can be normalized on the time scale to the time t_c .

The matrix equation for the coefficients of Eq. 2.16

then becomes:

$$\begin{bmatrix} 1 & 1 \\ \delta e^{\gamma l} & -\delta e^{-\gamma l} \end{bmatrix} \begin{bmatrix} A \\ B \end{bmatrix} = \begin{bmatrix} 0 \\ \frac{W}{2KA\delta} - \frac{t_c \bar{\epsilon}}{l} s \bar{T}_1 \end{bmatrix} \quad (2.24)$$

Solving Eq. 2.24 for the coefficients, substituting in Eq. 2.16, and solving for the temperature gives the temperature distribution at any point in terms of the temperature at the hot end:

$$\bar{T}_1(x, s) = \frac{W \sinh \delta x}{2KA\delta \cosh \delta l} - \frac{t_c \bar{\epsilon} s \sinh \delta x}{\delta l \cosh \delta l} \bar{T}_1(l, s) \quad (2.25)$$

Note that this expression is still in terms of the s domain. (We shall use the subscript 1 hereafter to denote the unperturbed solution.)

We can now solve for the unperturbed current by evaluating this expression at $x = l$ and substituting into the transform of Eq. 2.14. First, however, it will be convenient to normalize the transform variable in the following way:

$$\delta l = \sqrt{\frac{c}{K}} s l^2 = \sqrt{t_c s} \triangleq \sqrt{\mu} \quad (2.26)$$

and to define:

$$R_c \triangleq \frac{l}{2KA} = \text{the parallel thermal resistance of the couple} \quad (2.27)$$

and

$$z \triangleq \frac{\alpha^2}{\rho K} = \text{the thermoelectric figure of merit.} \quad (2.28)$$

Using these simplifications,

$$\bar{T}_1(l, \mu) = t_c R_c \frac{W \sinh \mu^{1/2}}{\mu^{3/2} [\cosh \mu^{1/2} + \bar{\epsilon} \mu^{1/2} \sinh \mu^{1/2}]} \quad (2.29)$$

This is the final result for the temperature variation of the hot junction in terms of the transform variable, u . The solution in the time domain can be determined by the conventional methods of contour integration to yield:

$$\hat{T}_1(t/t_0) = R_E W \left[1 - 2 \sum_{k=1}^{\infty} \frac{1}{\delta_k^2 (\bar{c}^2 \delta_k^2 + \bar{c} + 1)} e^{-\delta_k^2 t/t_0} \right] \quad (2.30)$$

where the δ_k 's are determined from the transcendental equation:

$$\tan \delta_k = \frac{1}{\bar{c} \delta_k} \quad (2.31)$$

It is now a simple step to get the unperturbed current by means of Eq. 2.14:

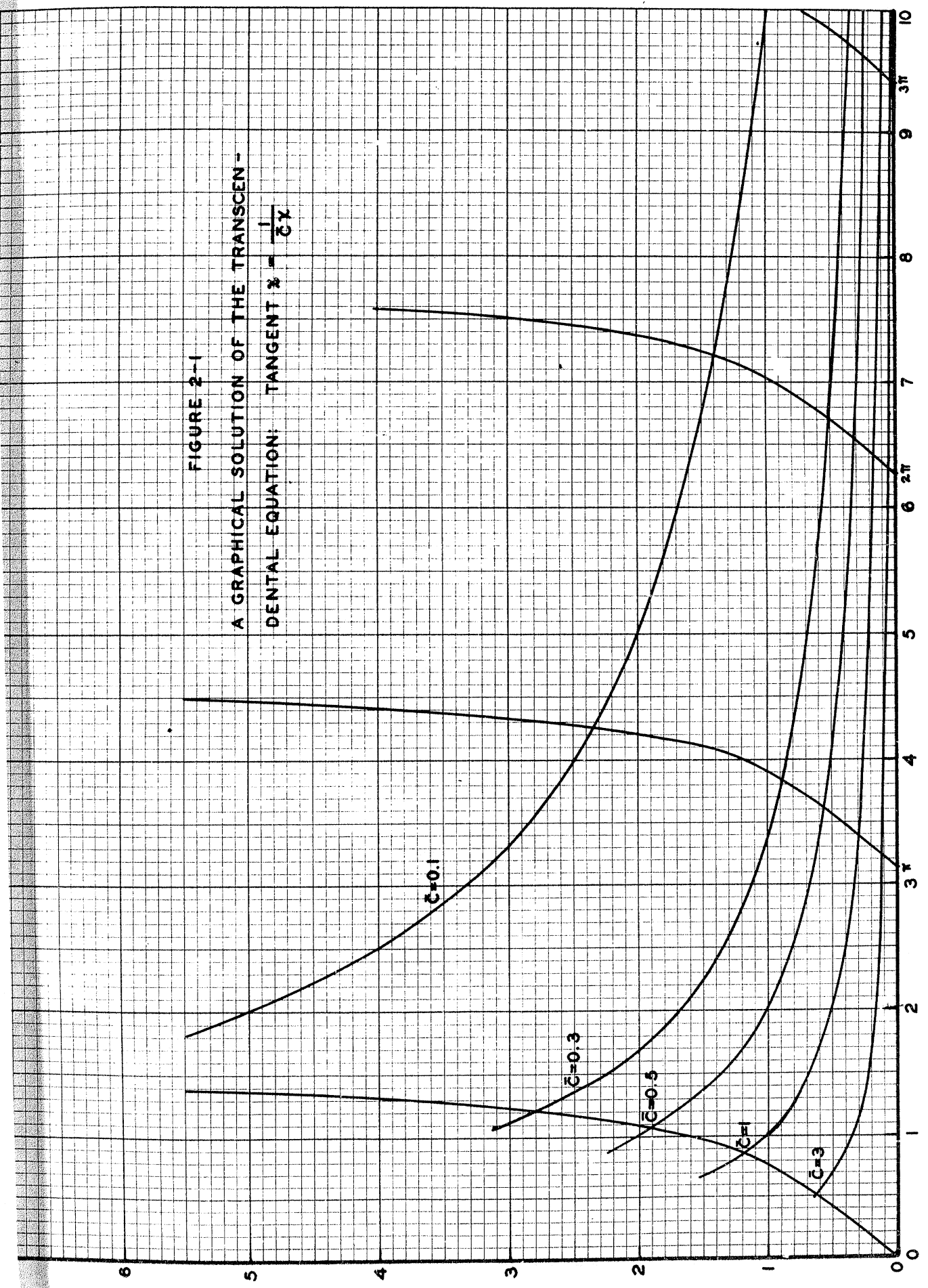
$$I_1(t/t_0) = I_{1,ss} \left[1 - 2 \sum_{k=1}^{\infty} \frac{1}{\delta_k^2 (\bar{c}^2 \delta_k^2 + \bar{c} + 1)} e^{-\delta_k^2 t/t_0} \right] \quad (2.32)$$

where

$$I_{1,ss} = \frac{\bar{z} W}{\alpha(m+1)} \quad (2.33)$$

This is the first of our desired results, namely, the current based upon the unperturbed (no-load) temperature distribution of the device. The form of the solution depends implicitly upon the normalized parameter \bar{c} through the roots of Eq. 2.31 and the residues of Eq. 2.32. A plot for the roots of Eq. 2.31 is given in Figure 2-1 for several values of \bar{c} and the values of the residues of Eq. 2.32 normalized to a base of .500 are given in Figure 2-2 as a function of \bar{c} . In order to indicate the relative magnitude of the first residue without actually plotting it, the percentage error in-

FIGURE 2-1
 A GRAPHICAL SOLUTION OF THE TRANSCENDENTAL EQUATION: $\tan x = \frac{1}{cx}$



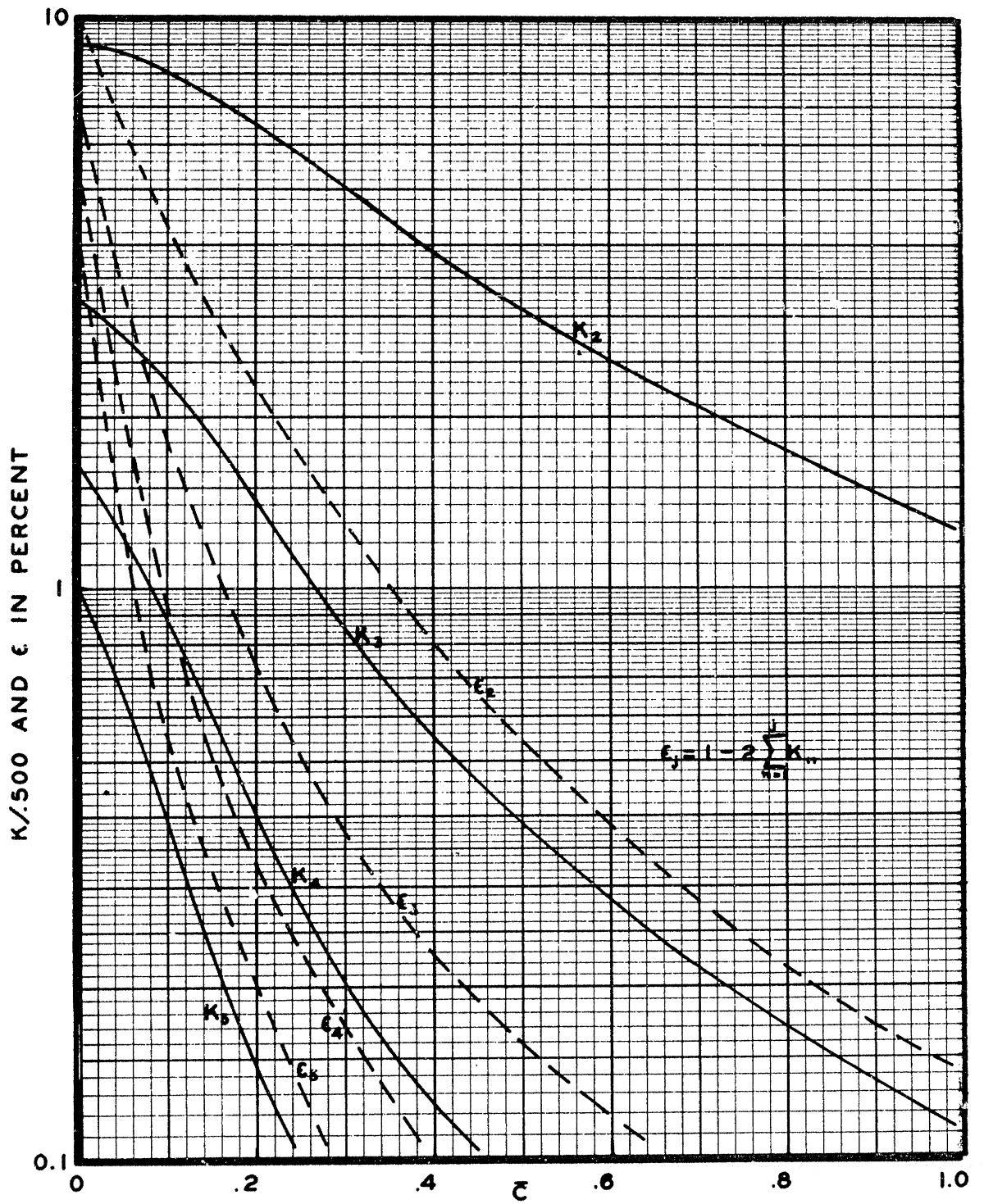


FIGURE 2 - 2
 THE RESIDUES FOR THE UNPERTURBED SOLUTION

troduced by breaking off the series of residues at any finite number of poles is shown. The percentage of error is defined at $t=0$, based on the steady state value of the unperturbed current.

By means of these two charts, the unperturbed current can be written by inspection. For instance, for $\bar{c} = .500$, $\delta_1 = 1.08$, $\delta_2 = 3.64$, $\delta_3 = 6.58$ from Figure 2-1 and from Figure 2-2,

$$K_2 = (.031)(.500) = .0155$$

$$K_3 = (.0038)(.500) = .0019.$$

From Figure 2-2, the error introduced by dropping the residues after K_3 is .16% or .0016 so that

$$K_1 = .500 - .0155 - .0019 - .0008 = .4818.$$

Therefore the unperturbed current for $c = .5$ can be written as:

$$\frac{I}{I_{ss}} = 1 - 2 \left[.4818 e^{-(1.08)^2 t/t_c} + .0155 e^{-(3.64)^2 t/t_c} + .0019 e^{-(6.58)^2 t/t_c} \right].$$

Note that the residues decrease so rapidly that the unperturbed current can be closely approximated by dropping all terms after the first residue, particularly for larger times. The maximum error introduced by such an approximation occurs for $t=0$. From the plot of the residues, it can be seen that this approximation becomes better as \bar{c} increases so that the solution for the unperturbed current becomes comparatively simple for larger values of \bar{c} . It is fortunate that this corresponds closely to the

practical case for it allows us to make use of the perturbation scheme with a minimum of effort.

The unperturbed current relation, Eq. 2.32, is a fictitious quantity as far as measurements in the laboratory are concerned since it describes the current which would flow on the assumption that there is no interaction between the temperature distribution and the flow of current. However, a very nice experimental check can be made of the results of this chapter by monitoring the temperature of the hot junction and checking the results with Eq. 2.30.* Figure 2-3 shows the calculated curve and the experimental points determined from the experimental model which had a measured \bar{c} of 0.304. The predicted temperature dependence for $\bar{c} = 0$ (i.e., neglecting the effect of the heater) is also indicated. One concludes from these results that the value of the normalized parameter, \bar{c} , has a dominating influence upon the time response of the device for values as small as 0.100. The results of Figure 2-3 are quite encouraging.

* For details of the experiment, see Appendix B.

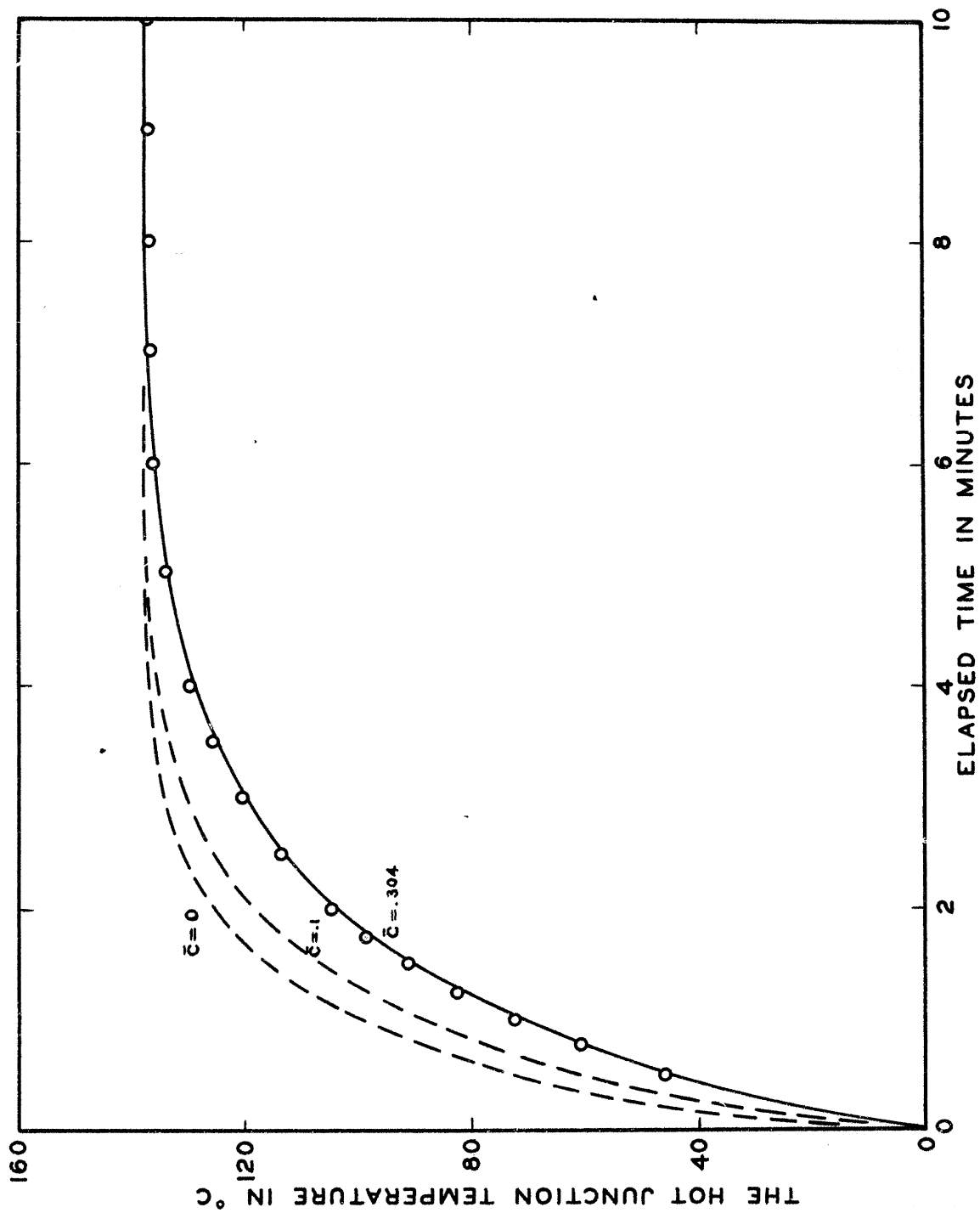


FIGURE 2-3. UNPERTURBED RESULTS FOR THE HOT JUNCTION TEMPERATURE

III. THE EFFECT OF A LOAD ON THE TRANSIENT BEHAVIOR

In Chapter II, we found a solution for the temperature distribution as a function of time under no-load conditions, and from this an "unperturbed" current was found. This neglected the non-linear effects and either a perturbation scheme or an iterative process must be used to approach a final solution. The former method was chosen because it offered the advantage of calculating the successive corrections to the solution which was obtained in Chapter II, rather than to recalculate the entire solution. Either method must be examined to see if it converges rapidly enough to be used. After the matter of convergence is taken care of, we can proceed to set up a perturbation process and then seek a solution for the problem under consideration. It proves to be an advantage to remain in the s domain until the final answer is formulated and then invert back to the time domain. Finally, we compare the results of Chapter II and Chapter III with the experimental results.

Going back to the equations which were set up in Chapter I and solved for the special case of $I = 0$ and $\tau = 0$ in Chapter II, we have (for $I \neq 0$, $\tau = 0$):

$$\kappa A \frac{\partial^2 \bar{T}}{\partial x^2} - c A \frac{\partial \bar{T}}{\partial t} + \frac{\rho}{A} I^2 = 0 \quad (3.1)$$

Since we already have a solution for the current, we can substitute into this expression and solve for the

perturbed temperature distribution due to this current. Before proceeding, however, let us define the following Laplace transformations:

$$\beta_1(s) \triangleq \mathcal{L}[I_1^2(t)] \quad (3.2)$$

$$\phi_1(s) \triangleq \mathcal{L}[I_1(t) \bar{T}_{l_1}(t)] = \frac{R_{eq}}{\alpha} (m+1) \beta_1(s) \quad (3.3)$$

The transformation of Eq. 3.1 then gives (with the correct boundary condition for $t=0$):

$$\frac{\partial^2 \bar{T}}{\partial x^2}(x, s) - \frac{c}{k} s \bar{T}(x, s) = \frac{p}{kA^2} \beta_1(s) \quad (3.4)$$

for which the solution in the s domain is:

$$\bar{T}(x, s) = A e^{\sqrt{x}} + B e^{-\sqrt{x}} + \frac{p}{A^2 c s} \beta_1(s) \quad (3.5)$$

subject to the transformed boundary conditions, Eqs. 2.11 and 1.10:

$$\bar{T}(0, s) = 0 \quad (3.6)$$

$$P_h(s) = \frac{W}{s} = \alpha \int [I_1(t) \bar{T}_{l_1}(t)] + 2kA \left. \frac{\partial \bar{T}}{\partial x}(s) \right|_{x=l} + c_0 A_0 l_0 \bar{T}_{l_2}(s). \quad (3.7)$$

Here \bar{T}_{l_2} is the total temperature after the perturbation is taken into account. We shall denote the perturbation itself by primes (so that $\bar{T}_{l_2} = \bar{T}_{l_2} + \bar{T}'_{l_2}$). Eq. 3.7 can also be written as:

$$\left. \frac{\partial \bar{T}}{\partial x}(s) \right|_{x=l} = \frac{W}{2kAs} - \frac{c_0 A_0 l_0}{2kA} s \bar{T}_{l_2} - \frac{\alpha}{2kA} \phi_1(s) \quad (3.8)$$

The matrix equation for the coefficients can be set up as in Chapter II resulting in:

$$\begin{bmatrix} 1 & 1 \\ \gamma e^{s\ell} & -\gamma e^{-s\ell} \end{bmatrix} \begin{bmatrix} A \\ \theta \end{bmatrix} = \begin{bmatrix} -\frac{\rho}{A^2 c s} \beta_1(s) \\ \frac{W}{2\kappa A s} - \frac{\alpha}{2\kappa A} \phi_1(s) - \frac{c_0 A_0 l_0}{2\kappa A} s \bar{T}_{R_2}(s) \end{bmatrix} \quad (3.9)$$

which can be arranged to give:

$$\begin{bmatrix} 1 & 1 \\ \gamma e^{s\ell} & -\gamma e^{-s\ell} \end{bmatrix} \begin{bmatrix} A \\ B \end{bmatrix} = \begin{bmatrix} 0 \\ \frac{W}{2\kappa A s} - \frac{l_0}{\ell} c \bar{T}_{R_2}(s) \end{bmatrix} - \begin{bmatrix} \frac{\rho}{A^2 c s} \beta_1(s) \\ \frac{\alpha}{2\kappa A} \phi_1(s) \end{bmatrix} \quad (3.10)$$

A comparison of these results with Eq. 2.24 immediately suggests a perturbation scheme since only the subtractive matrix on the right-hand side of Eq. 3.10 has changed with the perturbation. In fact, it is possible to define the coefficients as a set of additive terms, each corresponding to a perturbation matrix on the right. The total solution is then composed of the superposition of these solutions. Such a system might work very well if higher perturbations were desired, although it may become very lengthy if it is necessary to go to the time domain and then back to the transform domain between each successive perturbation. In theory, it is possible to appeal to the convolution integral but in practice the equations become too difficult to handle by these methods.

Before we can proceed with our proposed perturbation, we note that the first right-hand term of Eq. 3.10 contains a term in the junction temperature and therefore the matrices are not explicit in terms of the temperature

as they stand. This prevents us from setting up a perturbation system until we solve explicitly for the temperature. To do this, we can solve for the coefficients A and B, substitute back into Eq. 3.5, evaluate the result at $x=l$, and then find an expression for the temperature, \bar{T}_{l_2} . This latter step yields:

$$\left[1 + t_c \bar{c} \frac{s \sinh \delta l}{\delta l \cosh \delta l} \right] \bar{T}_{l_2} = \left[\frac{W \sinh \delta l}{2 \kappa A s \delta \cosh \delta l} \right] + \left[\frac{P}{A^2 c s} - \frac{P}{A^2 c s \cosh \delta l} - \frac{R_{eq} (m+1) \sinh \delta l}{2 \kappa A \delta \cosh \delta l} \right] \beta_1(s) \quad (3.11)$$

Comparing this result with Eq. 2.25 shows that we have already solved this relation for $\beta_1(s) = 0$ in Chapter II so that the solution for the additive perturbation now becomes:

$$\left[1 + t_c \bar{c} \frac{s \sinh \delta l}{\delta l \cosh \delta l} \right] \bar{T}'_{l_2} = \left[\frac{P}{A^2 c s} - \frac{P}{A^2 c s \cosh \delta l} - \frac{R_{eq} (m+1) \sinh \delta l}{2 \kappa A \delta \cosh \delta l} \right] \beta_1(s) \quad (3.12)$$

where the prime indicates the additive perturbation. Making use of the definitions and groupings used in Chapter II, we have:

$$\bar{T}'_{l_2}(u) = R_{eq} R_c t_c \left[\frac{(\cosh \sqrt{u} - 1) - (m+1) \sqrt{u} \sinh \sqrt{u}}{u (\cosh \sqrt{u} + \bar{c} \sqrt{u} \sinh \sqrt{u})} \right] \beta_1(u) \quad (3.13)$$

Up to this point, we have said little concerning $\beta(s)$ except to define the notation. Before we proceed fur-

ther, it is necessary to specify $\beta(s)$ more fully. The term defined as $\beta(s)$ is, in the transform domain, the convolution of the unperturbed current with itself or, in terms of the time domain, the transform of the square of the unperturbed current. In this analysis, we shall prefer to treat $\beta(s)$ in the latter sense as it is clearer to see what is happening physically and therefore allows us to make simplifying assumptions in terms of the physical model.

It was noted in Chapter II that the residues of the solution for the unperturbed current decrease rapidly for the larger values of \bar{c} . It was shown from Figure 2-2 that the retention of one residue for $c = .300$ gives an accuracy loss of 1% at $t=0$ (which is the point of maximum error) so that, for $c = .300$ (i.e., for the practical case), the unperturbed current can be approximated very closely for $t > 0$ by the first residue. Then, from Eq. 2.32, it follows that

$$\frac{I_1(t/t_0)}{I_{1,ss}} \doteq 1 - \frac{2}{\delta_1^2 (\bar{c}^2 \delta_1^2 + \bar{c} + 1)} e^{-\delta_1^2 t/t_0}$$

or,

$$\frac{I_1^2(t/t_0)}{I_{1,ss}^2} \doteq 1 - \frac{4}{\delta_1^2 (\bar{c}^2 \delta_1^2 + \bar{c} + 1)} e^{-\delta_1^2 t/t_0} + \frac{4}{\delta_1^4 (\bar{c}^2 \delta_1^2 + \bar{c} + 1)^2} e^{-2\delta_1^2 t/t_0} \quad (3.14)$$

This transforms to:

$$\beta(\mu) = \frac{1}{\mu} - \frac{4}{\delta_1^2 g(\delta_1)} \cdot \frac{1}{\mu + \delta_1^2} + \frac{4}{\delta_1^4 g^2(\delta_1)} \cdot \frac{1}{\mu + 2\delta_1^2} \quad (3.15)$$

where the following definition has been made for convenience:

$$g(\delta) \triangleq \bar{c}^2 \delta^2 + \bar{c} + 1 \quad (3.16)$$

Combining the results of Eqs. 3.13 and 3.15 yields the total perturbation result in the transform domain:

$$\frac{1}{t, R_E R_{eq}} \frac{\bar{T}'_{k_2}}{I_{1,ss}^2} = \left\{ \frac{1}{\mu} - \frac{4}{\delta^2 g(\delta) [\mu + \delta^2]} + \frac{4}{\delta^4 g^2(\delta) [\mu + 2\delta^2]} \right\} \times \left\{ \frac{(\cosh \mu^{1/2} - 1) - (m+1) \mu^{1/2} \sinh \mu^{1/2}}{\mu (\cosh \mu^{1/2} + \bar{c} \mu^{1/2} \sinh \mu^{1/2})} \right\} \quad (3.17)$$

For convenience, the inversion of this result will be handled in three separate groupings, each one corresponding to a term of the above product and then the numerical results will be combined in like terms. But first it is convenient to utilize the final value theorem to obtain the steady state (and maximum) perturbation. Application of the final value theorem to Eq. 3.17 yields:

$$\lim_{t \rightarrow \infty} \left[\frac{1}{R_E R_{eq}} \cdot \frac{\bar{T}'_{k_2}(t)}{I_{1,ss}^2} \right] = \lim_{\mu \rightarrow 0} \left[\frac{1}{t, R_E R_{eq}} \cdot \frac{\bar{T}'_{k_2}(\mu)}{I_{1,ss}^2} \right] = -(m+1/2) \quad (3.18)$$

or,

$$\lim_{t \rightarrow \infty} \left[\bar{T}'_{k_2} \right] = -(m+1/2) R_E R_{eq} I_{1,ss}^2 = R_E W_Z \frac{(m+1/2)}{(m+1)} \bar{T}_{k_1,ss} \quad (3.19)$$

From this result, an obvious test for the convergence of the perturbation process is that

$$\left| R_E W_Z \frac{(m+1/2)}{(m+1)} \right| < 1 \quad (3.20)$$

and the degree of the inequality gives us some idea of the relative degree of convergence. For the experimen-

tal model described in Appendices A and B, this test of convergence yielded $|.075|$ for a matched load ($m=1$). The perturbation process is fully justified for this case. Note that the criteria of convergence is directly related to the efficiency of the device through the "figure of merit" parameter z .

The inversion of Eq. 3.17 is lengthy but follows the conventional methods of inversion by contour integration in the complex domain. The perturbation introduces a pole of second order which makes the task of calculating the residues quite tedious. The second order pole enters since we have assumed (from Eq. 2.14) that the current and the hot junction temperature are related by constants of the system and therefore have the same mathematical dependence. It follows from this that a second order pole is introduced when the current-temperature product is taken. In other words, it is the Peltier effect which introduces the second order pole in the perturbation. It is the residue of the second order pole which proves quite useful in the calculation of device settling time.

Retaining the method of grouping which was begun in Eq. 3.17, the final result is:

$$\frac{I_2'}{I_{1,ss}^2} = \frac{\alpha R_c}{(m+1)} \left\{ \left[-(m + 1/2) + 2 \sum_{k=1}^{\infty} \frac{(m+1+\bar{c}) \delta_k \sin \delta_k - 1}{\delta_k^2 g(\delta_k) \delta_k \sin \delta_k} e^{-\delta_k^2 t/\tau_c} \right] \right\}$$

$$\begin{aligned}
 & -\frac{4}{\delta_1^2 g(\delta_1)} \left[\frac{h(\delta_1) + f(\delta_1) \delta_1 \sin \delta_1}{2 \delta_1^2 g^2(\delta_1) \delta_1 \sin \delta_1} e^{-\delta_1^2 t/t_1} - 2 \frac{(m+1+\bar{c}) \delta_1 \sin \delta_1 - 1}{g(\delta_1) \delta_1 \sin \delta_1} \frac{t}{t_1} e^{-\delta_1^2 t/t_1} \right. \\
 & \quad \left. + 2 \sum_{k=2}^{\infty} \frac{(m+1+\bar{c}) \delta_k \sin \delta_k - 1}{a(\delta_k) \delta_k \sin \delta_k} e^{-\delta_k^2 t/t_1} \right] \\
 & + \frac{4}{\delta_1^2 g^2(\delta_1)} \left[-\frac{1}{2} \frac{(\cos \sqrt{2} \delta_1 - 1) + (m+1) \sqrt{2} \delta_1 \sin \sqrt{2} \delta_1}{\delta_1^2 (\cos \sqrt{2} \delta_1 - \bar{c} \sqrt{2} \delta_1 \sin \sqrt{2} \delta_1)} e^{-2 \delta_1^2 t/t_1} \right. \\
 & \quad \left. + 2 \sum_{k=1}^{\infty} \frac{(m+1+\bar{c}) \delta_k \sin \delta_k - 1}{b(\delta_k) \delta_k \sin \delta_k} e^{-\delta_k^2 t/t_1} \right] \quad (3.21)
 \end{aligned}$$

where the following groups of polynomials have been made for convenience in the numerical computation:

$$a(\delta) \triangleq \bar{c}^2 \delta^4 + (\bar{c} - \bar{c} \delta^2 + 1) \delta^2 - (1 + \bar{c}) \delta^2 \quad (3.22)$$

$$b(\delta) \triangleq \bar{c} \delta^4 + (1 + \bar{c} - 2 \bar{c}^2 \delta^2) \delta^2 - 2 \delta^2 (1 + \bar{c}) \quad (3.23)$$

$$\begin{aligned}
 f(\delta) \triangleq & 2 \bar{c}^3 (m+1) \delta^4 - \bar{c} [5 \bar{c}^2 + (m+3) \bar{c} - 2(m+1)] \delta^2 \\
 & - [3 \bar{c}^2 + (m+6) \bar{c} + (m+3)] \quad (3.24)
 \end{aligned}$$

$$g(\delta) \triangleq \bar{c}^2 \delta^2 + \bar{c} + 1 \quad (3.16)$$

$$h(\delta) \triangleq 5 \bar{c}^2 \delta^2 + 3 \bar{c} + 3 \quad (3.25)$$

This result appears to be quite formidable and indeed it is! Fortunately, however, the results can be simplified somewhat when $\bar{c} \geq .300$; in fact, this is the condition upon which we were justified to make the approximations leading to this result so that this is certainly not restrictive. The numerical solutions for several cases have been listed in Appendix C so that

the reader may gain some appreciation of the relative magnitudes of the residues.

The first simplification which is evident from a comparison of the numerical work listed in Appendix C is that the terms corresponding to the "correlation" between the residues at the poles of the unperturbed current are quite negligible. By "correlation", we mean the effect that a pole in the unperturbed solution has upon any of the residues of the poles in the perturbed solution excepting the pole considered. As an example, let us pick $\bar{c} = 0.304$ and $m = 1$ for which the temperature perturbation becomes (from Appendix C):

$$\frac{1}{R_{\epsilon} R_{\epsilon\gamma}} \frac{\bar{I}_{\epsilon_1}'}{I_{1,ss}^2} = -1.500 + .4929 e^{-\delta_1^2 t/t_0} + .0405 e^{-\delta_2^2 t/t_0} + .000147 e^{-\delta_3^2 t/t_0} \\ + .000326 e^{-\delta_4^2 t/t_0} + 3.718 t/t_0 e^{-\delta_1^2 t/t_0} + 1.005 e^{-2\delta_1^2 t/t_0} \quad (3.26)$$

In deriving this, we have assumed that in the unperturbed solution the residues at all poles except the first one were negligible. This is also true in the perturbation so that we can conclude that if the residue at a pole is dropped in the unperturbed solution, the residue at the corresponding pole in the perturbation can be neglected and the "correlation" or effect on the residues at other poles in the perturbation can also be neglected. Moreover, the error introduced by these approximations in the perturbation is less than the error

introduced by the corresponding approximations made in the unperturbed solution, although this error is a function of both the normalized parameter \bar{c} and the normalized load parameter m . In general, these assumptions become more valid as \bar{c} increases. Eq. 3.26 then simplifies to:

$$\frac{1}{R_E R_{eq}} \frac{\bar{I}_{Ez}'}{I_{Ez}'} = -1.500 + .4929 e^{-\delta_1^2 t/\tau_1} + 3.718 t/\tau_1 e^{-\delta_1^2 t/\tau_1} + 1.005 e^{-2\delta_1^2 t/\tau_1} \quad (3.27)$$

The above relations can be expressed in terms of the current by means of Eq. 2.14. The results of Eq. 3.21 are plotted in Figure 3-1 for several values of \bar{c} .

Having found the complete solution to our problem, we are now in a position to compare the results with the experimental evidence. The details of the experimental model are covered in Appendix A; to retain continuity we shall only refer to certain aspects here. A bismuth telluride p-n junction was used with a copper heater and connecting strap. The cold junction was kept at ice-water temperature and a power input of 4.15 watts was applied to give a temperature differential of 140°C. across the junction under no-load conditions. The load voltage was recorded as a function of time for various loadings of the generator and several runs were made for each loading. The heater was designed to give as small a value of the normalized parameter, \bar{c} , as was practically possible; the experimentally determined value of \bar{c} was determined to be 0.304. The parameters of the system

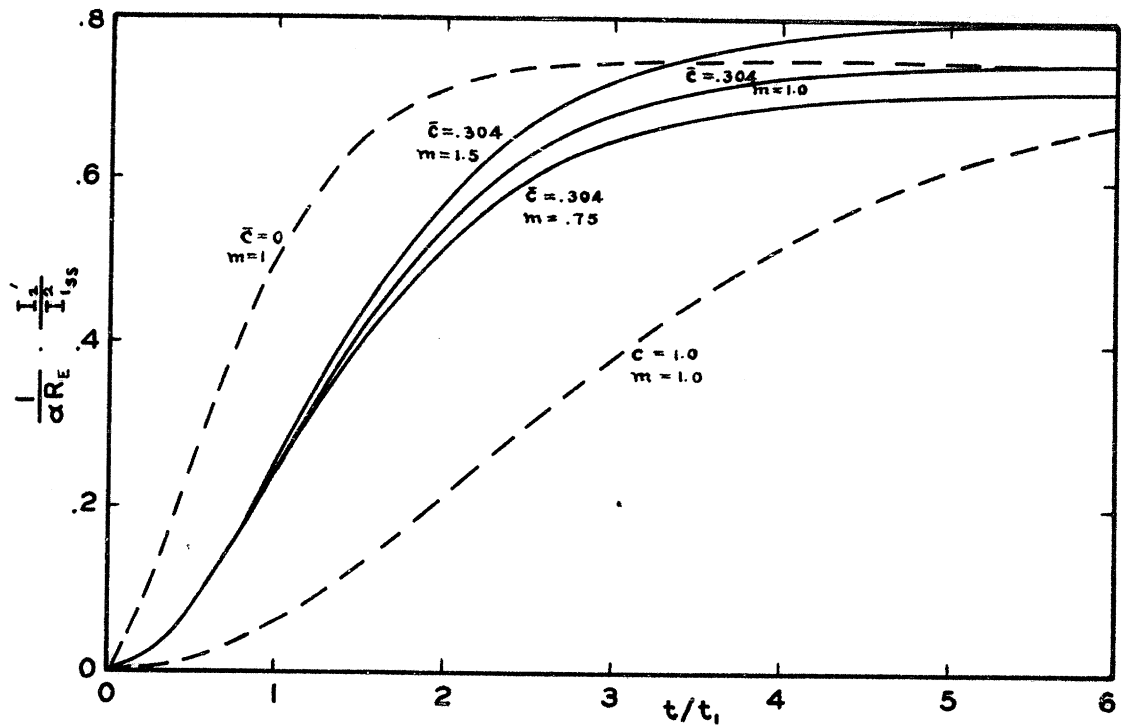


FIGURE 3-1
THE PERTURBATIONS OF THE JUNCTION CURRENT

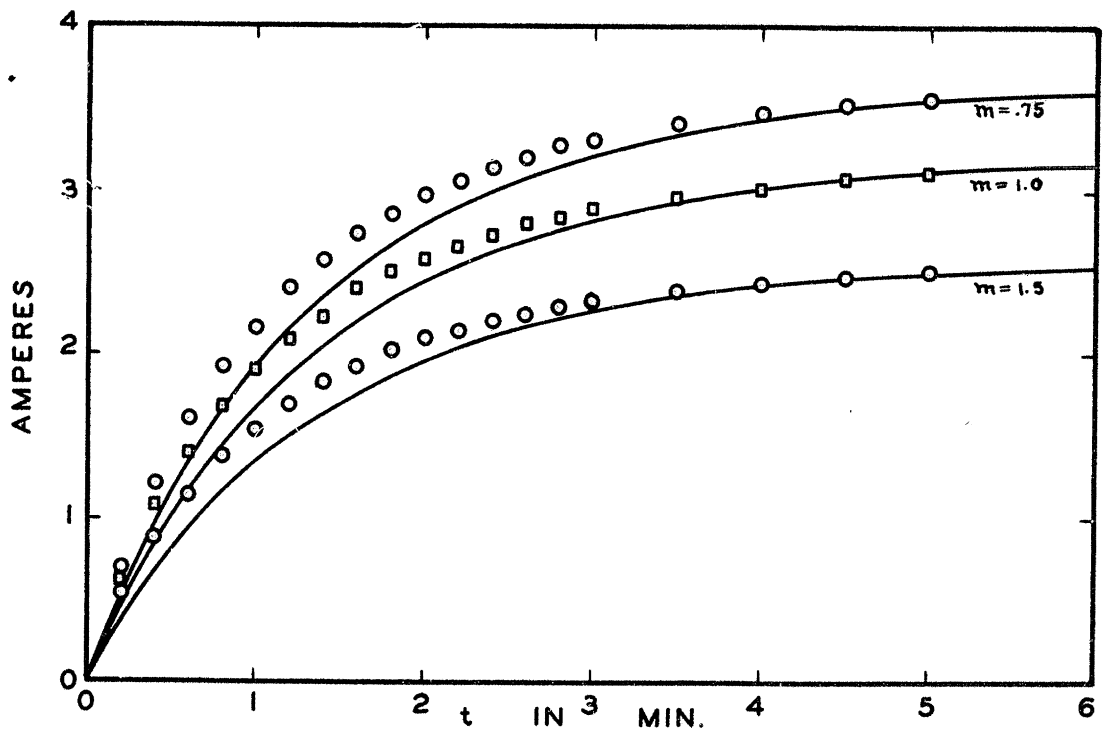


FIGURE 3-2
A COMPARISON OF THE RESULTS WITH THE EXPERIMENT

which were used in the calculated results were obtained by using the averaged values corresponding to the steady state temperature. This is covered in more detail in Appendix B.

The results of the calculations are compared with the results of the experiment in Figure 3-2 for three different loadings of the generator. The results seem to agree fairly well; however, the results are not in as close agreement as the comparison of the open circuit hot junction temperature in Chapter II. Note that the discrepancies occur in the short-time region and are consistent from one load condition to another. Since the perturbation results are the only change in the theory from Chapter II to Chapter III, this would seem to point to the perturbation as the source of error. But the perturbation results are effective mainly for longer time intervals than the region in which the discrepancies occur. The temperature distribution which was found in Chapter II is in good agreement with experimental results; therefore we should not overlook the parameters which link the current to the temperature.

From the results previously obtained, it was found that the current output of the device is directly proportional to the effective value of the thermoelectric figure-of-merit parameter, z . This parameter was determined for the experimental model and the temperature de-

pendence is included in Appendix B. It was found that α varies considerably with temperature, steadily decreasing as the temperature increases. The overall effect is that the output current is higher than that which is predicted for the lower temperatures and as the temperature of the device approaches the steady state value, the predicted values and the experimental values converge. In other words, the discrepancies which are observed can be explained on the basis of the inaccuracies in the constant parameter assumption (which were not present in the experimental check of Chapter II).

IV. THE SETTLING TIME OF THE SYSTEM

It is often desirable to be able to predict in advance how long it will take for a device to come within a preset tolerance of its steady state value. This can be defined as a settling time, t_s , in which the system attains, say, 95% of its steady state current output under load conditions. Earlier in this work, it was shown that both the unperturbed solution and the perturbation can be closely approximated for times $t/t_s > 1$ for the practical case. Furthermore, for these longer times, the parameters of the system are not changing very rapidly and can be assumed to be near a "quasi-static" average value. Therefore we have disposed of both of the troubles which have bothered us in Chapter III.

Making use of the simplifications which were considered in Chapter II, we can drop all the terms from the unperturbed solution except the constant term and the one involving the first residue so that:

$$\frac{I_1}{I_{1,ss}} \doteq 1 - 2 K_1 e^{-\delta_1^2 t/t_s} \quad . \quad (\text{from Eq. 2.32})$$

The simplified perturbation from Chapter III is:

$$\frac{I_2'}{I_{1,ss}} = \frac{\alpha R_L}{(\gamma + 1)} I_{1,ss} \left[-(\gamma + 1/2) + K_{11} e^{-\delta_1^2 t/t_s} + K_{s1} t/t_s e^{-\delta_1^2 t/t_s} + K_{s1} e^{-2\delta_1^2 t/t_s} \right] \quad (4.1)$$

where the residues are numbered to correspond to the respective terms of Eq. 3.21.

First of all, we recognize (from the convergence criterion of Chapter III) that the perturbation is small compared to the unperturbed current. Also, for long times, the term of the form $\alpha e^{-\delta^2 t/t_c}$ dominates the perturbation as long as its residue is sufficiently large in comparison to the residues of the other terms. Actually, the residue K_1 in Eq. 4.1 exceeds the residue K_{31} for $\bar{c} > 1.5$ but since the exponential decay rate is double, our approximation still holds. In accordance with these approximations we can write for the long time approximation:

$$\frac{I}{I_{1ss}} \doteq 1 - 2K_1 e^{-\delta^2 t/t_c} - \frac{\alpha R_E}{m+1} I_{1ss} \left[(m+1/2) - K_{31} t/t_c, e^{-\delta_1^2 t/t_c} \right] \quad (4.2)$$

or, since
$$I_{1ss} = \frac{zW}{\alpha(m+1)} \quad , \quad (2.33)$$

$$\frac{I}{I_{1ss}} \doteq 1 - 2K_1 e^{-\delta^2 t/t_c} - \frac{zR_E W}{(m+1)^2} \left[(m+1/2) - K_{31} t/t_c, e^{-\delta_1^2 t/t_c} \right] \quad (4.3)$$

where, from Chapter III,

$$K_1 = \frac{1}{\delta_1^2 g(\delta_1)} \quad (\text{from Eq. 3.21})$$

$$K_{31} = \frac{\theta \left[(m+1+\bar{c}) \delta_1 \sin \delta_1 - 1 \right]}{\delta_1^2 g^2(\delta_1) \delta_1 \sin \delta_1} \quad (\text{from Eq. 3.21})$$

$$g(\delta) = \bar{c}^2 \delta^2 + \bar{c} + 1, \quad (3.16)$$

and δ_1 is determined by the first root of:

$$\tan \delta = \frac{1}{\bar{c} \delta} \quad (2.31)$$

A settling time, t_s , can now be calculated on the basis of the time required for the system to come to

95% of the steady state operation point. Table 4-1 shows the results of the calculations (slide rule accuracy) for various values of the normalized parameters and a comparison with the settling time calculated without considering the perturbation terms is indicated.

From Table 4-1, it will be noted that the agreement with the observed values is good. Furthermore, note that this method predicts the settling time as a function of the loading and of the power input. For instance, if the power input were increased to 10 watts (assuming

\bar{c}	m	WITHOUT THE PERTURBATION t_s/t_i	WITH THE PERTURBATION		OBSERVED RESULTS t_s (min.)
			t_s/t_i	t_s (min.)	
0.304	.75	1.98	1.864	4.23	4.25
"	1.00	1.98	1.824	4.14	4.15
"	1.50	1.98	1.886	4.28	4.30
1.00	1.00	4.03	3.78		
3.00	1.00	10.0	9.40		

TABLE 4-1

DEVICE SETTLING TIMES FOR CONSTANT POWER INPUT

that the materials could withstand such an implied temperature differential), the device settling time is reduced to 8.43 minutes for $\bar{c} = 3$ and $m = 1$.

Let us see why the settling time of the generator should be less with a load than it is for the open cir-

circuit condition. From the perturbation results of Chapter III, we saw that the interaction of the current and the temperature distribution does not begin to take place immediately after the initial instant except for very small values of \bar{c} . Therefore the temperature has a chance to build up almost as fast as in the unloaded case. However, the interaction causes the steady state operating temperature to be less (through the Peltier effect) than that of the open circuit case so that the device comes to within 5% of the steady state operating point in a shorter time. Stated differently, the initial rate at which the current transient builds up is approximately equal for the two cases but, under load, the steady state operating point is lower so that the settling time must be less for the loaded generator (assuming no overshoot).

It is also interesting to note that the optimum loading ratio on the basis of the settling time is near the point $m=1$. An exact expression for the optimum value of m is not easy to obtain, however. The solution can be found from a trial-and-error type of solution for each value of \bar{c} . It is not clear from physical reasoning why the optimum value should be at a loading ratio of unity.

This completes the work which has been done on the initial large signal transients in the thermoelectric generator. The mathematical solution has been set up

and solved, and a perturbation scheme was adopted to obtain a solution in the presence of non-linearities. The results were shown to be only as good as the assumptions which were made to derive the solution. Several simplifying assumptions were made and the settling time of the device was considered with satisfactory results.

REMARKS

In general, the results of this work have been encouraging. The problem has been set up in detail and a solution has been obtained after several simplifying assumptions were made. Since the results can be only as valid as the assumptions, we shall proceed to consider these assumptions and to discuss some possible ways to avoid making them.

In setting up the mathematical description of the device, it was assumed that the flow of heat was one-dimensional and the elements were assumed to be homogeneous in composition. These assumptions were valid for the model which was used in the laboratory; in general, it is possible that they may not be valid. The first assumption presents no great difficulty in setting up the problem since the gradient could have been used just as well in the differential equations. The complexities in handling such equations and attempting to obtain a solution would be so great, however, as to make the problem quite impractical. In fact, it would probably be easier to find a solution for the one-dimensional case and then attempt to explain the effects of the other dimensional dependences. If the elements are homogeneous in a piece-wise manner, the problem could have been broken up into separate parts. Again, this makes the

calculations difficult. If the homogeneity is not so clearly defined, the problem cannot be solved in an exact manner.

The parameters of the system were assumed to be independent of the temperature and it was shown that this assumption introduced some error in the final results. If this assumption were not made, however, the differential equations would not have constant coefficients and the methods used in this analysis would no longer be valid. In addition, the variation of the parameters with the temperature cannot be represented by a simple function throughout the entire temperature range of operation if this range is of any extent. The problem would possibly be sectioned into separate parts, each part valid over a given range. It may be possible to program a computer for the problem on this basis.

We made the additional assumption in Chapter II that the Thomson heat term was negligible compared to the Peltier heat term. For certain materials and over certain temperature ranges, this assumption may have to be revised. The difficulty in retaining this term in the differential equations is that the equations no longer have a straight-forward analytical solution. It may be possible to formulate a method whereby the final solution can be perturbed to account for the Thomson heat.

With these assumptions, the results of this work are quite satisfactory for the system which was considered. Both the current transient and the settling time of the system can be predicted closely if the above assumptions are valid. The work concerning the settling time of the device brings up some surprising results. It was found that the settling time was less for the generator under load than under open circuit conditions. From the results, it appears that the settling time is at a minimum when the generator impedance and the load impedance are equal. These results have only been checked with one system, however, and there is certainly opportunity to expand this work.

APPENDIX A: DETAILS OF THE EXPERIMENTAL MODEL

This section is added to provide some of the details of the experimental model which was used for a comparison with the theory of Chapters II, III, and IV. The block diagram of the experiment is shown in Figure A-1 and is self-explanatory. The coolant used was water and the liquid bath was kept at ice-water temperature by means of stirring crushed ice in the bath. The temperature of the heat sink had a tendency to rise slightly as the power was applied to the heater. It was found that this drift of the base temperature was not too large, however, and was approximately linear with time during the first few minutes of each run. Corrections were applied to the results on this basis.

The generator is shown by an actual-size drawing in Figure A-2 and the details of the heater assembly are shown in Figure A-3. Considerable time was spent in designing the heater so that a small, compact unit could be used which would (1) have negligible radiation losses, (2) provide equi-temperature surfaces with a negligible time lag, (3) have negligible electrical and thermal resistance, and (4) handle five watts of electrical power continuously. The normalized specific heat, \bar{c} , of the heater assembly was calculated on a mass basis instead of by Eq. 2.22. The mass of the solder on the heater

was included with the mass of the copper heater and this total mass was used to compute the normalized specific heat of the assembly. The error introduced by this approximation is small if the ratio of copper to solder is large.

The calculations for \bar{c} are as follows:

mass of Bi_2Te_3 arms = .26.28 gm.

specific heat of $\text{Bi}_2\text{Te}_3 = 0.0372 \text{ cal./gm.}^\circ\text{K}$

mass of heater assembly = 2.930 gm.
(including solder)

specific heat of copper = $0.1014 \text{ cal./gm.}^\circ\text{K}$

$$\bar{c} = \frac{C_{\text{Cu}}}{C_{\text{Bi}_2\text{Te}_3}} = \frac{(0.1014)(2.930)}{(0.0372)(26.28)} = 0.304$$

This is the value used in the calculations in this paper.

The maximum temperature at which the generator could be operated was limited by the materials used in the generator arms. It was found that the n-type material had a tendency to crack along the cleavage plane at a temperature of approximate-

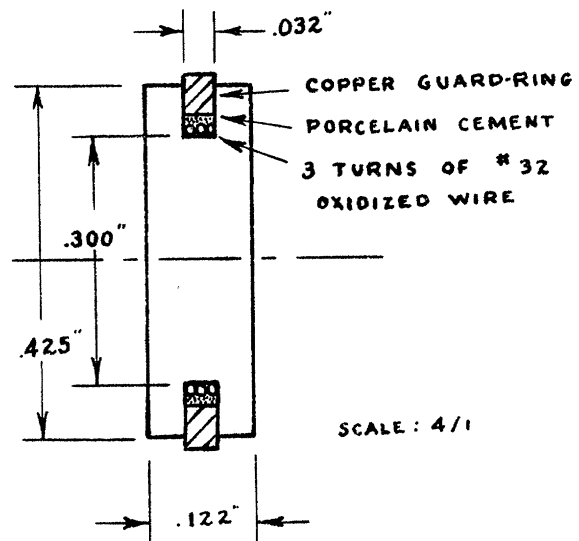


FIGURE A-3
DETAILS OF THE HEATER

ly 175°C. The tests described in this paper were run at a power level which gave a no-load hot junction temperature of 140°C. This made an allowance for a considerable drift in the base temperature and still permitted a margin of safety.

For each value of load resistance, several runs were taken to minimize the errors introduced by the recording system. A dynamic linearity test was then run on the recording system using an accurate millivoltmeter (Keithley Model 150 Micro-volt-ammeter) and the linearity was found to be rather poor at the higher recording level. A correction ratio was formulated and it was found that the component of error was proportional to the third power of the magnitude of the reading.

Another source of difficulty experienced in this system was that the heater resistance had a tendency to vary at random due to the inadequate insulation between turns. This effect was quite troublesome but was minimized by matching the transformer to the heater. The thin oxide-type insulation was chosen to provide a path of high thermal conductance from the heater winding to the faces of the heater. It was found that the time lag between the time of the application of a current pulse to the heater winding and the beginning of a temperature rise at the heater face was about 0.12 seconds which is quite negligible in this case.

APPENDIX B: DETERMINATION OF THE AVERAGE PARAMETERS

In this experiment, the same material with different dopings was used for the two arms of the generator. The theory developed in this paper makes approximations which are the most valid for this case since we have assumed that the parameters have the same temperature dependence and hence can be treated as averaged parameters with a minimum of error.

There are two main approaches to the problem of averaged parameters. One method is to measure the parameters of each material separately and then average the results. The other method is to determine the average values from measurements taken on the entire system. The first method was used to determine the averaged resistivity, ρ' , which was then checked by use of the second method. The second method was used to determine α' and κ' and several checks were made by using the first method.*

To determine the effective values of the thermal conductivity, κ , and the Seebeck coefficient, α , the power input to the heater was varied keeping the cold junction temperature constant at 0°C. and the hot junction temperature (under no-load conditions) was recorded after reaching a steady state value. Assuming that all

* The measurements of α and κ of the individual materials are taken from readings taken for the author by Henry Lyden and from the work of Dr. P. E. Gray.

the power delivered to the system is conducted to the cold junction (i.e., no radiation losses, etc.), we can write:

$$P_{in} = \kappa' A \frac{\Delta T_{SS}}{l} \quad (B.1)$$

and

$$V_{o.c.} = \alpha' \Delta T_{SS} \quad (B.2)$$

where κ' and α' are the effective values. The results of this test are shown in Figure B-1 together with the check points taken from the measurements on the individual samples ($\alpha' = \frac{1}{2} [|\alpha_a| + |\alpha_b|]$, $\kappa' = \frac{1}{2} [\kappa_a + \kappa_b]$).

The resistivity of the p- and n-type material used is shown in Figure B-2 and the volt-ampere characteristic of the generator is shown in Figure B-3. The latter results are for steady state operation and a constant power input of 4.15 watts which corresponds to a no-load hot junction temperature of 140°C. From the slope of the line of Figure B-3, the effective resistance, R_{eq} , is found to be 9.33 milliohms which corresponds to $\rho' = 1.95$ millohm-cm. From Figure B-2, the effective value of ρ' is calculated to be (for 140°C.):

$$\rho' = \frac{\rho_a + \rho_b}{2} = \frac{1.81 + 2.11}{2} = 1.96 \text{ m}\Omega\text{-cm.}$$

so that

there is substantial agreement between the methods used.

By combining the results of these methods, an effective "figure-of-merit" parameter, z' , can be defined as:

$$z' = \frac{(\alpha')^2}{\rho' \kappa'}$$

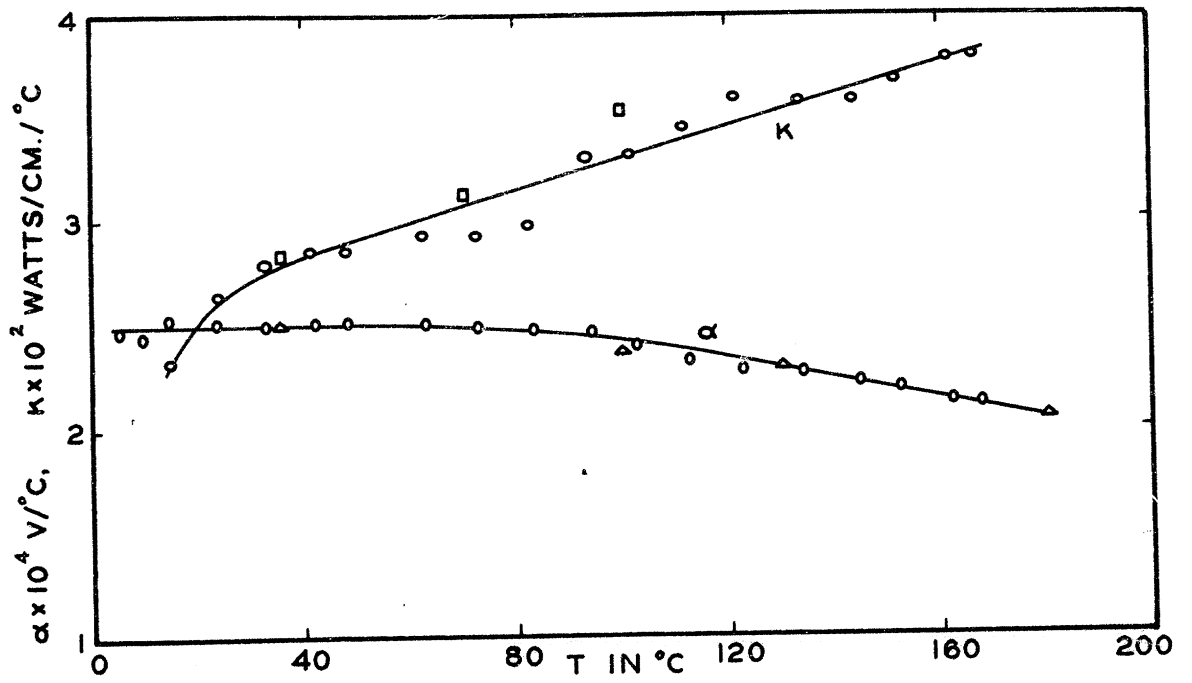


FIGURE B-1
THE EFFECTIVE α AND κ OF THE GENERATOR ARMS

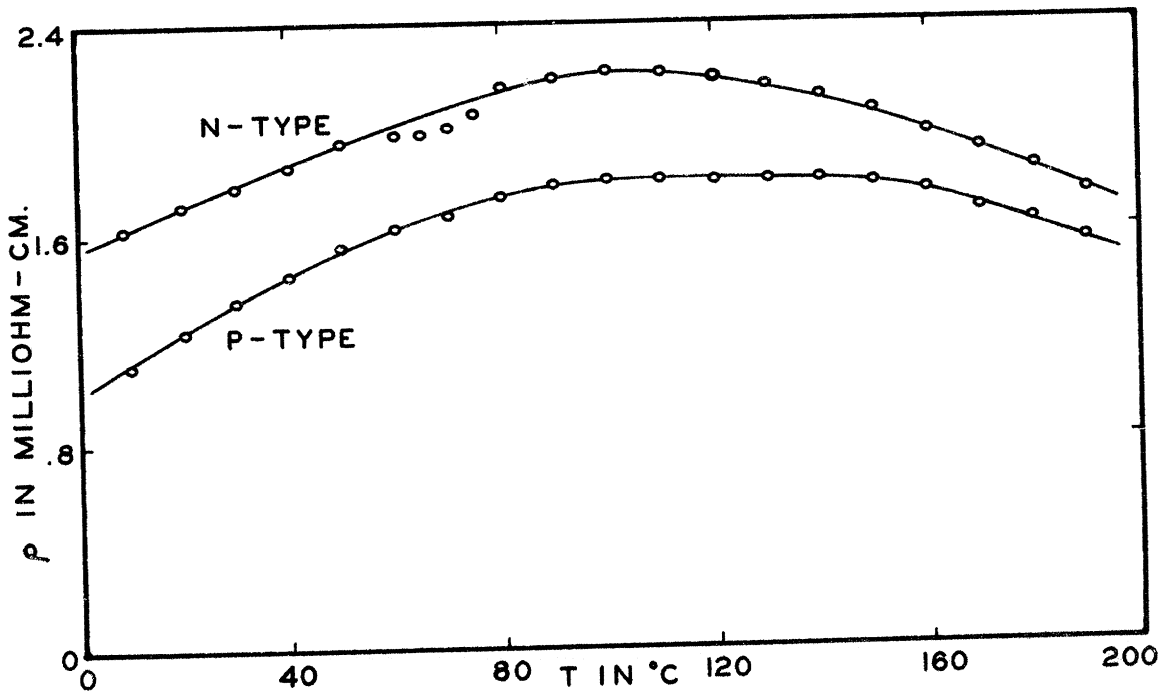


FIGURE B-2
THE RESISTIVITY OF THE BISMUTH TELLURIDE USED

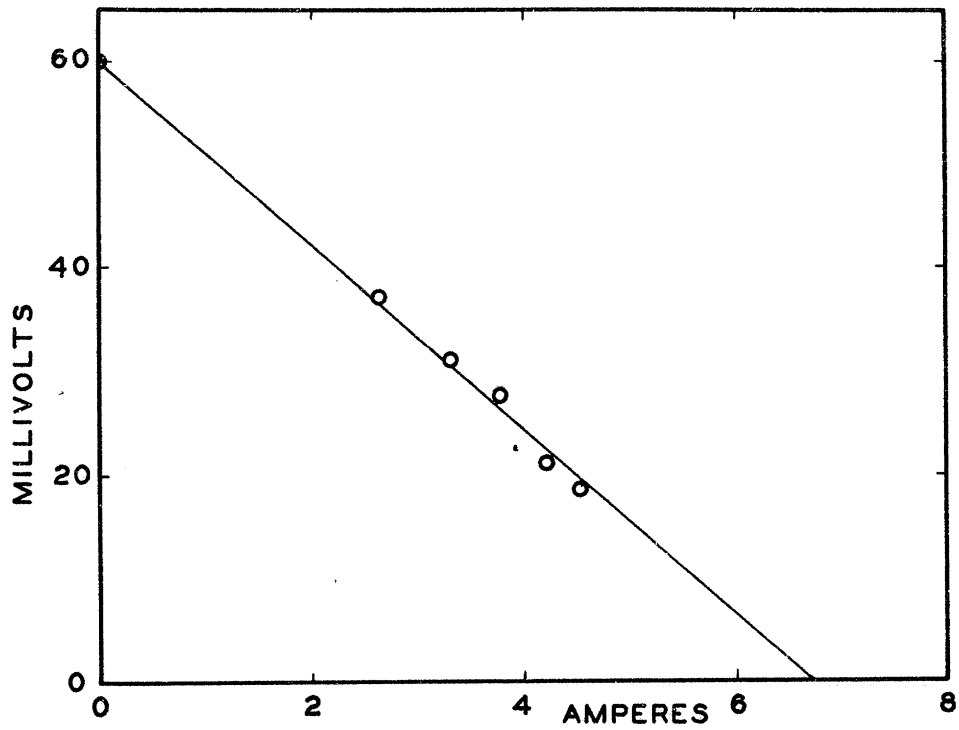


FIGURE B-3
THE VOLT-AMPERE CHARACTERISTIC FOR
A CONSTANT POWER INPUT

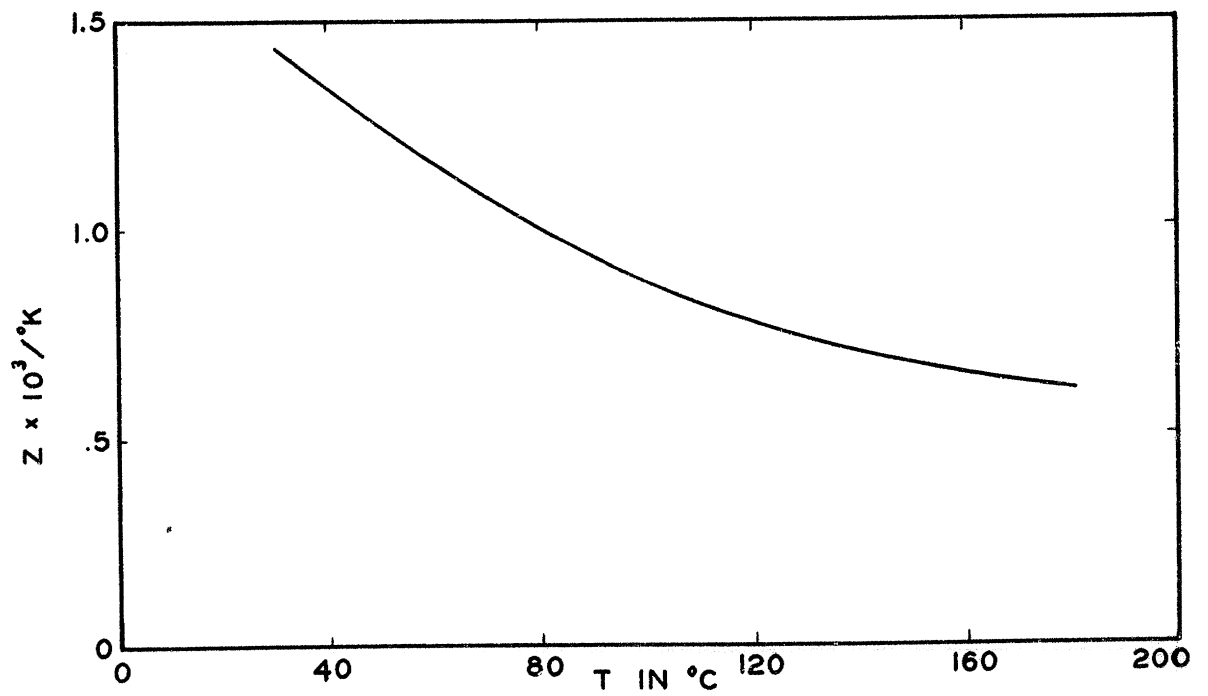


FIGURE B-4
THE EFFECTIVE Z OF THE GENERATOR

and is plotted in Figure B-4. It is this variation with temperature which accounts for the discrepancies in the results cited in Chapter III.

Using the results of this section and the notation used in the main body of this paper, we can now calculate the values for the experimental model corresponding to the steady state temperature.

$$\alpha' = 2.25 \text{ } \mu\text{VOLTS}/^{\circ}\text{K}$$

$$K' = 36.0 \text{ MILLIWATTS}/\text{CM.}^{\circ}\text{K}$$

$$\rho' = 1.95 \text{ MILLIOHM-CM.}$$

$$\bar{\epsilon}' = 0.72 \times 10^{-3}/^{\circ}\text{K}$$

$$R_E = l/2KA = 33.3 \text{ }^{\circ}\text{K}/\text{WATT}$$

$$R_{eq} = \rho' l/A = 9.33 \text{ MILLIOHMS}$$

$$t_1 = cl^2/K' = 136 \text{ SEC} = 2.27 \text{ MIN.}$$

The above values are the ones which are used in this paper.

APPENDIX C: A PARTIAL LIST OF RESIDUES
FOR THE COMPLETE SOLUTION

The numerical values of the residues for the results of Chapter II and Chapter III are included in this section for some arbitrary values of \bar{c} together with the values for \bar{c} and m corresponding to the experimental model. These values are included to provide some idea of relative magnitudes to the reader.

After the numerical computation, it is more convenient to group the results of Eqs. 2.32 and 3.21 into the following form:

$$\frac{I}{I_{1,ss}} = 1 - 2 \left[H_1 e^{-\delta_1^2 t/t_1} + H_2 e^{-\delta_2^2 t/t_1} + H_3 e^{-\delta_3^2 t/t_1} + H_4 e^{-\delta_4^2 t/t_1} \right]$$

$$- \frac{\alpha R_e}{m+1} I_{1,ss} \left[(m+1/2) - H_5 e^{-\delta_5^2 t/t_1} - H_6 e^{-\delta_6^2 t/t_1} - H_7 e^{-\delta_7^2 t/t_1} - H_8 e^{-\delta_8^2 t/t_1} \right. \\ \left. - H_9 t/t_1 e^{-\delta_9^2 t/t_1} - H_{10} e^{-2\delta_{10}^2 t/t_1} \right].$$

The numerical results in Table C-1 are listed using the above notation.

TABLE C-1

THE NUMERICAL RESULTS FOR THE RESIDUES OF EQ. C-1

\bar{c}	m	H_1	H_2	H_3	H_4
0.00		.4053	.0450	.0162	.00827
0.304		.4690	.0253	.00401	.00104
1.00		.4931	.00620	.000556	.000119
3.00		.4990	.000963		
\bar{c}	m	H_5	H_6	H_7	H_8
0.00	1.00	1.0656	.004176	.001546	.001038
0.304	.75	.4327	-.03676	-.001642	-.000295
"	1.00	.4929	-.0405	.000147	.000326
"	1.50	.6131	-.0480	-.00236	-.000388
1.00	1.00	.1523	.000386	.000006	.000005
3.00	1.00	.0381			
\bar{c}	m	H_9	H_{10}		
0.00	1.00				
0.304	.75	3.0666	.8153		
"	1.00	3.7176	1.0050		
"	1.50	5.0197	1.3844		
1.00	1.00	2.1112	1.3477		
3.00	1.00	0.8865	1.4613		

REFERENCES

1. Ioffe, A.F., Semiconductor Thermoelements and Thermoelectric Cooling, London: Infosearch, Ltd., 1957.
2. Borrego, J.M., Lyden, H.A., and Blair, J., The Efficiency of Thermoelectric Generators, WADC TN 58-200, M.I.T. Industrial Liaison Office, 1958.
3. Sherman, B., Heikes, R.R., and Ure, R.W., "Calculation of Efficiency of Thermoelectric Devices", Journal of Applied Physics, 31, (January) 1960, pp. 1-16.
4. Gray, P.E., The Dynamic Behavior of Thermoelectric Devices, New York, John Wiley & Sons, Inc., 1960.
5. Burshstein, A.I., "An Investigation of the Steady State Heat Flow through a Current-Carrying Conductor", Soviet Physics--Technical Physics, 2, (July) 1957, pp. 1397 ff.
6. Carslaw, H.S., and Jaeger, J.C., Conduction of Heat in Solids, London: Oxford University Press, 1959.
7. Gardner, M.F., and Barnes, J.L., Transients in Linear Systems, New York: John Wiley & Sons, Inc., 1942, ch.8.
8. Churchill, R.V., Operational Mathematics, New York: McGraw-Hill Book Co., 1958.